

Biosensing Platform Based on Fluorescence Resonance Energy Transfer from Upconverting Nanocrystals to Graphene Oxide**

Cuiling Zhang, Yunxia Yuan, Shiming Zhang, Yuhui Wang, and Zhihong Liu*

Fluorescence resonance energy transfer (FRET) is recognized as a sensitive and reliable analytical technique and has been widely used in biological assays.^[1] To obtain improved FRET efficiency and analytical performance, it is of continuing interest to search for new energy donor–acceptor pairs. In the past few years, the use of anti-Stokes fluorophores including upconverting phosphors (UCP) and multiphoton-excited dyes as energy donors which can be excited in the near-infrared (NIR) region has successfully circumvented the problem of autofluorescence and scattering of light arising from biological substances.^[2,3] This has made it possible to directly conduct FRET-based assays in biological samples. More recently, graphene, the newly emerging two-dimensional and zero-bandgap carbon nanomaterial, has attracted considerable attention in bioassays because of its unique electronic, mechanical, and thermal properties. In the pioneering work of Swathi et al., it was proposed through theoretical calculations that graphene could act as a super-quencher of organic dyes, as a result of nonradiative transfer of electronic excitation energy from dye excited states to the π system of graphene.^[4] The rate of this long-range resonance energy transfer was suggested to have a d^{-4} dependence on distance d , in sharp contrast to traditional FRET, for which the rate has a d^{-6} dependence. Inspired by this property, graphene and graphene oxide (GO) have been used as FRET acceptors with organic dyes and quantum dots as energy donors,^[5–11] in which both graphene and GO exhibit high efficiency in quenching the donor emission and thus provide good sensitivity. Herein we reveal energy transfer from UCP to GO and thus construction of a new biosensing platform which could be used to detect glucose directly in serum samples and extended to detection of other biologically significant molecules.

The previously reported FRET models based on graphene or graphene oxide all rely on the π – π stacking interaction between the carbon nanomaterial and nucleic acid chains, which bring the acceptor and donor (organic dyes or quantum

dots) into close proximity. We hereby tried a different model in which donor and acceptor are brought into FRET proximity through specific molecular recognition (Figure 1).

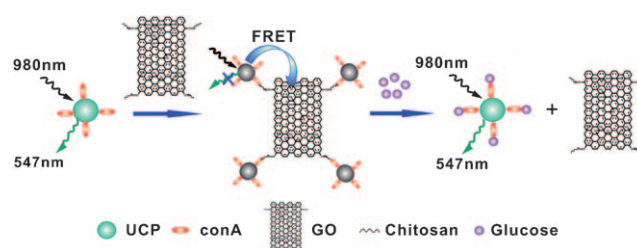


Figure 1. Schematic illustration of the UCP–GO biosensing platform and the mechanism of glucose determination.

We used GO as energy acceptor because the abundance of carboxy, hydroxy, and epoxy groups on the surface of GO sheets^[12] makes the material more water-soluble and also enables covalent conjugation with other molecules. Concanavalin A (conA) and chitosan (CS) were covalently attached to UCP and GO, respectively. The known tight binding of ConA with CS may bring UCP and GO into appropriate proximity and hence induce energy transfer. Thereafter, the FRET process is anticipated to be inhibited (in part) because of competition between glucose and CS for ConA, which could be the foundation of glucose sensing.

To realize such design, we first synthesized water-soluble NaYF₄:Yb,Er UCP nanocrystals modified with polyacrylic acid (PAA). Details of UCP synthesis are given in the Supporting Information. The fluorescence intensity of UCP remains unchanged under continuous 980 nm illumination for up to several hours, which suggests good photostability. Highly dispersible PAA-functionalized UCP particles with an average particle size of about 50 nm were obtained, which consisted of a dominant hexagonal phase and a small amount of cubic phase (Figure S1, Supporting Information). The UCP–ConA conjugate was prepared by an 1-ethyl-3-(3-dimethylaminopropyl) carbodiimide (EDC) coupling protocol, and successful conjugation was confirmed by UV/Vis spectroscopy (Figure S2, Supporting Information). Graphene oxide nanosheets were synthesized according to the reported method,^[6] and the obtained dispersion was dialyzed through semipermeable membranes to remove impurities. The products were characterized by the XRD pattern (Figure S3, Supporting Information), which exhibits the characteristic diffraction peak of GO at $2\theta = 10.58^\circ$. Chitosan molecules were attached to the surface of GO by EDC-mediated coupling, and FTIR spectra were recorded to characterize the chemical structure of GO and GO–CS conjugates (Figure S4,

[*] C. L. Zhang, Y. X. Yuan, S. M. Zhang, Y. H. Wang, Prof. Z. H. Liu
Key Laboratory of Analytical Chemistry for Biology and Medicine
(Ministry of Education), College of Chemistry and Molecular
Sciences, Wuhan University, Wuhan 430072 (P. R. China)
Fax: (+86) 27-6875-4067
E-mail: zhliu@whu.edu.cn

[**] The authors thank Prof. S. L. Chen for helping with the characterization of GO. We also acknowledge the financial support from the National Natural Science Foundation of China (Grant No. 21075094), and the Science Fund for Creative Research Groups (Grant Nos. 20621502 and 20921062)

Supporting information for this article is available on the WWW under <http://dx.doi.org/10.1002/anie.201100769>.

Supporting Information). The characteristic absorption peaks of GO were observed, including peaks for O–H at 3413, C=O at 1731, C=C at 1622, and C–O at 1092 cm^{-1} (Figure S4a, Supporting Information). For the GO–CS complex, characteristic peaks corresponding to the C=O stretching vibration (1631 cm^{-1}), C–N stretching vibration (1384 cm^{-1}), and the asymmetric and symmetric stretching vibrations of methyl groups (2938 and 2873 cm^{-1}) were observed (Figure S4b, Supporting Information). Notably, both the UCP–ConA and GO–CS complexes showed good dispersibility in aqueous solution, which ensured the stability and reliability of spectroscopic measurements.

The formation of GO–CS–ConA–UCP complex by interaction between CS and ConA was first verified with AFM measurements. The AFM height image shows that the thickness of the as-synthesized GO sheets was about 1 nm (Figure 2a). When UCP–ConA was mixed with GO–CS, the

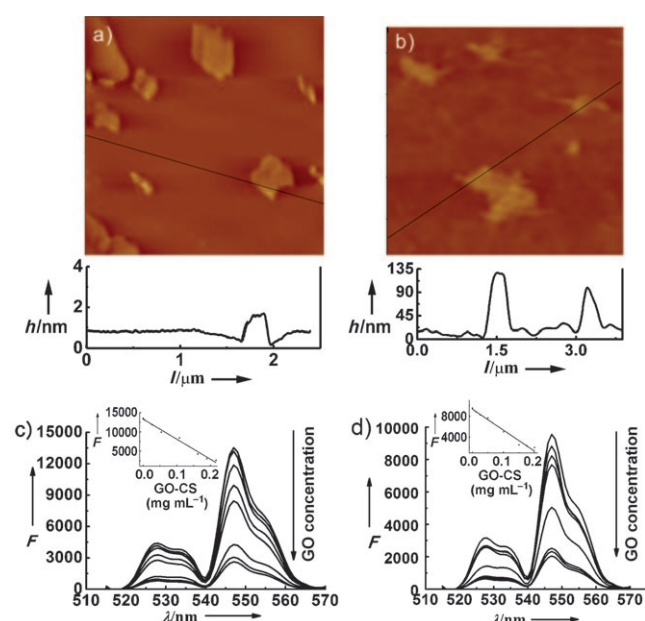


Figure 2. AFM images and height profiles of GO (a) and the GO–CS–ConA–UCP complex (b), and fluorescence titration of UCP–ConA (0.45 mg mL^{-1} UCP) by GO–CS with GO concentration ranging from 0 to 0.22 mg mL^{-1} in c) Tris–HCl buffer (0.01 M, pH 7.4) and d) human serum (20-fold diluted with Tris–HCl buffer) from which inherent glucose had been removed. Inset: linear relationship between fluorescence intensity of UCP and concentration of GO. Excitation wavelength: 980 nm.

heights of the complex were approximately 110 and 80 nm, which indicated that UCP was brought close to the GO surface (Figure 2b). Energy transfer from UCP to GO was then investigated by measuring the fluorescence quenching of UCP. On mixing GO–CS and UCP–ConA solutions (in 0.01 M Tris–HCl buffer, pH 7.4), the fluorescence intensity of UCP gradually decreased with increasing concentration of GO–CS (Figure 2c). The extent of fluorescence quenching linearly corresponded to the concentration of GO–CS (Figure 2c, inset). An overall degree of quenching of 81 % was obtained with a GO concentration of 0.22 mg mL^{-1} . Such a quenching

efficiency is somewhat lower than those reported with organic dyes as energy donor. This can be explained by the nature of UCP materials, in which only the emitters (rare earth ions) at or near the surface of particles can be quenched. For assays based on such a quenching–recovery model, higher fluorescence quenching rates are generally preferable in terms of determination sensitivity. Nonetheless, the extremely high luminescence efficiency of UCP nanocrystals still makes them competitive energy donors. As a kind of two-dimensional material with relatively large surface, adsorption of other substances (e.g., the UCP–ConA complex) on the surface of GO could be a concern that might cause false-positive signals. To rule out the possibility of nonspecific binding, a control experiment was done in which the UCP–ConA solution was mixed with 0.25 mg mL^{-1} of bare GO solution. No obvious signal change was observed in this case (Figure S5, Supporting Information), and this implies that no nonspecific adsorption of UCP–ConA on the GO surface occurs, and that the fluorescence quenching can be exclusively ascribed to recognition of CS by ConA.

Furthermore, we performed the above FRET experiments in human serum from which inherent glucose was removed by glucose oxidase (vide infra), with two purposes: 1) to take advantage of the NIR excitation of upconverting phosphors, that is, the ability to avoid background interference in a complex sample matrix like serum; 2) although the application of graphene materials in bioassay has been well demonstrated in the above-mentioned literature, the possibility of using them in such a complex biological sample matrix has not yet been explored. We found that, when using 20-fold diluted serum as medium, a FRET process that was nearly the same as that in aqueous buffer occurred (Figure 2d), except for a slight difference in the slope of the linear calibration (inset). Thus, the various biomolecules in the serum do not have a significant influence on either the FRET process or the optical measurements.

Considering the robustness of the FRET model shown by the above experiments, we subsequently determined glucose in serum medium. To preclude the influence of the inherent glucose in serum, it was decomposed with glucose oxidase followed by deactivating the enzyme. The resulting serum caused no significant signal alteration of the FRET sensor, that is, no inherent glucose was left (Figure S6, Supporting Information). Then external free glucose with varying concentrations was introduced to the sensor, which resulted in partial deconstruction of the GO–CS–ConA–UCP complex due to the stronger combination between glucose and ConA. Consequently, fluorescence of UCP donor was restored in a glucose concentration dependent manner (Figure 3). The plot of fluorescence intensity versus glucose concentration showed a linear calibration in the range from 0.56 to 2.0 μM . The limit of detection was 0.025 μM , calculated according to the $3s_b/m$ criterion, where m is the slope for the range of linearity used and s_b the standard deviation of a blank ($n = 11$). Such assay sensitivity is comparable to or even better than those of spectroscopic methods for glucose determination performed in aqueous solutions.^[13–17] The assay also exhibited good reproducibility, as shown by standard deviations from independent measurements (Figure 3b). As compared to the

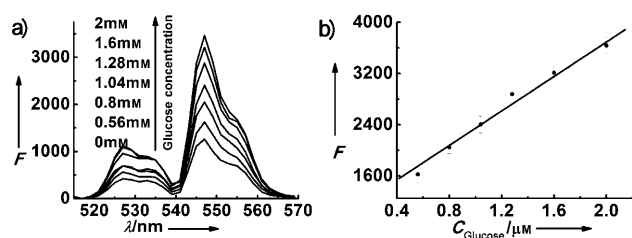


Figure 3. a) Fluorescence emission spectra of GO–CS–ConA–UCP complex in the presence of different concentrations of glucose (0.56–2.0 μM) in diluted serum. b) Linear relationship between donor fluorescence intensity and glucose concentrations. Excitation wavelength: 980 nm.

noncovalent π – π stacking between the ring structures in nucleobases and the hexagonal cells of graphene (or graphene oxide), the combination of target molecules on the surface of GO nanosheets through more robust and stable covalent bonds may contribute to analytical performance criteria such as sensitivity and precision, although it requires one more step for labeling. More importantly, the flexibility in covalent coupling reaction also laid a foundation for easily extending the FRET platform to other targets.

The specificity of the FRET sensor towards glucose was examined in control experiments in which other biomolecules including carbohydrate, protein, and amino acid were tested with procedures identical to the above assay. At a concentration equal to that of glucose (2.4 μM), the tested substances did not cause obvious restoration of donor fluorescence, except for mannose (Figure 4), which caused concentration-dependent recovery of UCP fluorescence (Figure S7, Supporting Information), as it is also recognized by conA.^[18] Nevertheless, the assay of glucose in human serum would not be affected, since mannose does not exist in mammalian blood.

To validate the expanded application of the UCP–GO FRET platform, a homogeneous hybridization model was adopted for ssDNA detection. UCP was first tagged to streptavidin (SA) by an EDC protocol, and successful

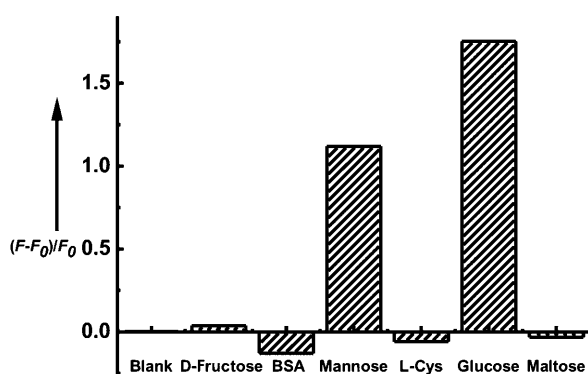


Figure 4. Variations in fluorescence intensity induced by different substances, all with a concentration of 2.4 μM . Blank represents the GO–CS–ConA–UCP complex, the fluorescence intensity of which is defined as F_0 , and F is the fluorescence intensity in the presence of tested substances. Experiments were conducted in 20-fold diluted (with Tris–HCl buffer) human serum from which inherent glucose had been removed. Excitation wavelength: 980 nm.

conjugation was confirmed by UV/Vis spectroscopy (Figure S8, Supporting Information). The UCP–SA complex was then linked to biotinylated ssDNA (5′-biotin-GAGTTAG-CACCCGCATAGTCAAGAT-3′) via the biotin (B)–SA bridge. On mixing the UCP–SA–B–ssDNA complex with increasing amounts of GO solution, the fluorescence of UCP was gradually quenched (Figure 5a), as a result of energy

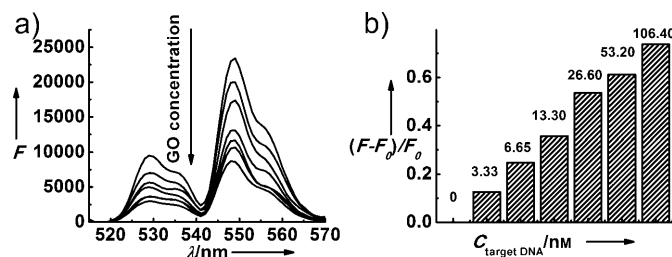


Figure 5. a) Fluorescence emission spectra of the UCP–SA–B–ssDNA complex in the presence of different concentrations of GO (0, 0.02, 0.05, 0.08, 0.10, 0.15, 0.2 mg mL^{-1}). b) Restoration of UCP fluorescence after incubation with target ssDNA (0, 3.33, 6.65, 13.3, 26.6, 53.2, 106.4 nM) in the presence of 0.2 mg mL^{-1} GO.

transfer from UCP to GO induced by the π – π stacking interaction between ssDNA and GO.^[5] In the presence of the complementary target ssDNA (5′-ATCTTGAC-TATGCGGGTGCTAACTC-3′), the stronger interaction of complementary chains disturbs the interaction between UCP–SA–B–ssDNA and GO, resulting in restoration of the fluorescence of UCP (Figure 5b).

In conclusion, we have constructed a novel sensor for glucose determination based on FRET from upconverting phosphors to graphene oxide. When excited with NIR light, the FRET sensor showed favorable analytical performance in a complex biological sample matrix. Unlike commonly used heterogeneous methods like ELISA, which need multiple separating steps, the proposed UCP–GO sensor is capable of homogeneously detecting glucose in serum samples without any background interference, so the UCP–GO FRET system could be a promising platform for biosensing. The covalent combination-based design can readily be extended to sensing of other biomolecules. This work may enrich the FRET technique and promote application of graphene materials in bioassay.

Experimental Section

Sensing of glucose: In a typical measurement, 0.27 mg mL^{-1} GO–CS solution was added to 3 mg mL^{-1} UCP–ConA in 20-fold diluted (with 0.01M Tris–HCl, pH 7.4) pretreated human serum. Thereafter, different concentrations of glucose were added to the above solution and the mixtures incubated for 1.5 h before measurement. Fluorescence emission of the donor was measured under excitation at 980 nm with a CW laser.

Detection of ssDNA: UCP (6.4 mg) was attached to SA (1.1 mg) in 8 mL 2-(*N*-morpholino)ethanesulfonic acid (MES, 0.01M, pH 6.06) containing 3.2 mg EDC and 9.6 mg *N*-hydroxysulfosuccinimide (Sulfo-NHS), and then biotinylated ssDNA (biotin in fourfold molar excess of SA) was added to the UCP–SA conjugate to form UCP–SA–B–ssDNA complex. In a typical hybridization procedure,

0.20 mg mL⁻¹ GO was added to the solution of UCP-SA-B-ssDNA complex. Thereafter, different concentrations of target ssDNA were added and the mixtures incubated for 1.5 h at 37 °C before measurement. Fluorescence emission of the donor was recorded under excitation at 980 nm with a CW laser.

Received: January 30, 2011

Revised: March 4, 2011

Published online: June 8, 2011

Keywords: analytical methods · biosensors · FRET · graphene · nanoparticles

- [1] a) S. Tyagi, F. R. Kramer, *Nat. Biotechnol.* **1996**, *14*, 303–308; b) B. Schuler, W. A. Eaton, *Curr. Opin. Struct. Biol.* **2008**, *18*, 16–26; c) N. Hildebrandt, L. J. Charbonnière, M. Beck, R. F. Ziesse, H. G. Löhmansröben, *Angew. Chem.* **2005**, *117*, 7784–7788; *Angew. Chem. Int. Ed.* **2005**, *44*, 7612–7615; *Angew. Chem. Int. Ed.* **2005**, *44*, 7612–7615; d) E. A. Jares-Erijman, T. M. Jovin, *Nat. Biotechnol.* **2003**, *21*, 1387–1395.
- [2] a) K. Kuningas, T. Rantanen, T. Ukonaho, T. Lövgren, T. Soukka, *Anal. Chem.* **2005**, *77*, 7348–7355; b) L. Wang, R. Yan, Z. Huo, L. Wang, J. Zeng, J. Bao, X. Wang, Q. Peng, Y. D. Li, *Angew. Chem.* **2005**, *117*, 6208–6211; *Angew. Chem. Int. Ed.* **2005**, *44*, 6054–6057; c) K. Kuningas, T. Ukonaho, H. Pääkkilä, T. Rantanen, J. Rosenberg, T. Lövgren, T. Soukka, *Anal. Chem.* **2006**, *78*, 4690–4696; d) T. Rantanen, H. Pääkkilä, L. Jämsen, K. Kuningas, T. Ukonaho, T. Lövgren, T. Soukka, *Anal. Chem.* **2007**, *79*, 6312–6318; e) K. Kuningas, H. Pääkkilä, T. Ukonaho, T. Rantanen, T. Lövgren, T. Soukka, *Clin. Chem.* **2007**, *53*, 145–146; f) T. Rantanen, M. L. Jarvenpää, J. Vuojola, K. Kuningas, T. Soukka, *Angew. Chem.* **2008**, *120*, 3871–3873; *Angew. Chem. Int. Ed.* **2008**, *47*, 3811–3813; g) S. Jiang, Y. Zhang, *Langmuir* **2010**, *26*, 6689–6694.
- [3] a) R. Wahlroos, J. Toivonen, M. Tirri, P. Hänninen, *J. Fluoresc.* **2006**, *16*, 379–386; b) A. R. Clapp, T. Pons, I. L. Medintz, J. B. Delehanty, J. S. Melinger, T. Tiefenbrunn, P. E. Dawson, B. R. Fisher, B. O'Rourke, H. Mattoussi, *Adv. Mater.* **2007**, *19*, 1921–1926; c) L. Z. Liu, G. H. Wei, Z. H. Liu, Z. K. He, S. Xiao, Q. Q. Wang, *Bioconjugate Chem.* **2008**, *19*, 574–579; d) L. Z. Liu, M. Shao, X. H. Dong, X. F. Yu, Z. H. Liu, Z. K. He, Q. Q. Wang, *Anal. Chem.* **2008**, *80*, 7735–7741; e) L. Z. Liu, X. H. Dong, W. L. Lian, X. N. Peng, Z. H. Liu, Z. K. He, Q. Q. Wang, *Anal. Chem.* **2010**, *82*, 1381–1388.
- [4] a) R. S. Swathi, K. L. Sebastian, *J. Chem. Phys.* **2008**, *129*, 054703; b) R. S. Swathi, K. L. Sebastian, *J. Chem. Phys.* **2009**, *130*, 086101.
- [5] C. H. Lu, H. H. Yang, C. L. Zhu, X. Chen, G. N. Chen, *Angew. Chem.* **2009**, *121*, 4879–4881; *Angew. Chem. Int. Ed.* **2009**, *48*, 4785–4787; *Angew. Chem. Int. Ed.* **2009**, *48*, 4785–4787.
- [6] H. F. Dong, W. C. Gao, F. Yan, H. X. Ji, H. X. Ju, *Anal. Chem.* **2010**, *82*, 5511–5517; F. Yan, H. X. Ji, H. X. Ju, *Anal. Chem.* **2010**, *82*, 5511–5517.
- [7] H. X. Chang, L. H. Tang, Y. Wang, J. H. Jiang, J. H. Li, *Anal. Chem.* **2010**, *82*, 2341–2346.
- [8] S. J. He, B. Song, D. Li, C. F. Zhu, W. P. Qi, Y. Q. Wen, L. H. Wang, S. P. Song, H. P. Fang, C. H. Fan, *Adv. Funct. Mater.* **2010**, *20*, 453–459.
- [9] Y. Wang, Z. H. Li, D. H. Hu, C. T. Lin, J. H. Li, Y. H. Lin, *J. Am. Chem. Soc.* **2010**, *132*, 9274–9276.
- [10] H. J. Jang, Y. K. Kim, H. M. Kwon, W. S. Yeo, D. E. Kim, D. H. Min, *Angew. Chem.* **2010**, *122*, 5839–5843; *Angew. Chem. Int. Ed.* **2010**, *49*, 5703–5707.
- [11] C. H. Lu, J. Li, J. J. Liu, H. H. Yang, X. Chen, G. N. Chen, *Chem. Eur. J.* **2010**, *16*, 4889–4894.
- [12] X. Y. Yang, X. Y. Zhang, Z. F. Liu, Y. F. Ma, Y. Huang, Y. S. Chen, *J. Phys. Chem. C* **2008**, *112*, 17554–17558.
- [13] O. J. Rolinski, D. J. S. Birch, L. J. McCartney, J. C. Pickup, *J. Photochem. Photobiol. B* **2000**, *54*, 26–34.
- [14] M. Dweik, S. A. Grant, *Sens. Trans. J.* **2008**, *3*, 71–79.
- [15] B. Tang, L. H. Cao, K. H. Xu, L. H. Zhuo, J. C. Ge, Q. L. Li, L. J. Yu, *Chem. Eur. J.* **2008**, *14*, 3637–3644.
- [16] P. Wu, Y. He, H. F. Wang, X. P. Yan, *Anal. Chem.* **2010**, *82*, 1427–1433.
- [17] R. Gill, L. Bahshi, R. Freeman, I. Willner, *Angew. Chem.* **2008**, *120*, 1700–1703; *Angew. Chem. Int. Ed.* **2008**, *47*, 1676–1679.
- [18] H. Lis, N. Sharon, *Chem. Rev.* **1998**, *98*, 637–674.